

ČESKÉ VYSOKÉ UČENÍ TECHNICKÉ V PRAZE  
FAKULTA STROJNÍ  
ÚSTAV MATERIÁLOVÉHO INŽENÝRSTVÍ



BAKALÁŘSKÁ PRÁCE

Bioaktivní vrstvy slitin Ti připravené na implantátech s nízkým  
elastickým modulem technologií nadzvukové kinetizace

Bioactive Ti-based coatings on low elastic modulus substrates by cold  
kinetic spray

AUTOR: Vojtěch Lukeš

STUDIJNÍ PROGRAM: Výroba a ekonomika ve strojírenství

VEDOUCÍ PRÁCE: Ing. Jan Čížek Ph.D.

PRAHA 2021



# ZADÁNÍ BAKALÁŘSKÉ PRÁCE

## I. OSOBNÍ A STUDIJNÍ ÚDAJE

Příjmení: **Lukeš** Jméno: **Vojtěch** Osobní číslo: **482590**  
Fakulta/ústav: **Fakulta strojní**  
Zadávající katedra/ústav: **Ústav materiálového inženýrství**  
Studijní program: **Výroba a ekonomika ve strojírenství**  
Studijní obor: **Technologie, materiály a ekonomika strojírenství**

## II. ÚDAJE K BAKALÁŘSKÉ PRÁCI

Název bakalářské práce:

**Bioaktivní vrstvy Ti připravené na implantátech s nízkým elastickým modulem technologií nadzvukové kinetizace**

Název bakalářské práce anglicky:

**Bioactive Ti coatings on low elastic modulus substrates by cold kinetic spray**

Pokyny pro vypracování:

Cílem této pilotní studie je nanosení vrstev Ti na připravené substráty z hořčíkové slitiny pomocí technologie nadzvukové kinetizace.

Jednotlivé kroky: 1. vypracovat rešerši o základních charakteristikách technologie studené kinetizace, 2. vypracovat rešerši o materiálech pro implantáty kostní tkáně, 3. provést depozici vrstev Ti na zvolený podkladový materiál (nejspíše AZ31), 4. posoudit mikrostrukturu a fázově-chemické složení vyhotovených vrstev.

Seznam doporučené literatury:

- Papyrin, Kosarev, Klinkov, Alkhimov, Fomin: Cold Spray Technology. Elsevier Science, 2006.
- Schmidt, Assadi, Gartner, Richter, Stoltenhoff, Kreye, Klassen: From Particle Acceleration to Impact and Bonding in Cold Spraying. Journal of Thermal Spray Technology, 18 (5–6), 2009, 794–808.
- Heimann, Lehmann: Bioceramic coatings for medical implants. Wiley, 2015.
- Wang, Zhang: Cold-spray coatings on magnesium and its alloys. Surface Modification of Magnesium and its Alloys for Biomedical Applications. Woodhead Publishing, 2015.
- Narayanan, Park, Lee: Surface Modification of Magnesium and its Alloys for Biomedical Applications. Woodhead Publishing, 2015.

Jméno a pracoviště vedoucí(ho) bakalářské práce:

**prof. RNDr. Petr Špatenka, CSc., ústav materiálového inženýrství FS**

Jméno a pracoviště druhé(ho) vedoucí(ho) nebo konzultanta(ky) bakalářské práce:


**Ing. Jan Čížek, Ph.D., Ústav fyziky plazmatu AV ČR, v. v. i.**

Datum zadání bakalářské práce: **04.04.2021**

Termín odevzdání bakalářské práce: **25.07.2021**

Platnost zadání bakalářské práce: \_\_\_\_\_

  
prof. RNDr. Petr Špatenka, CSc.  
podpis vedoucí(ho) práce

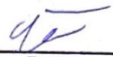
  
prof. RNDr. Petr Špatenka, CSc.  
podpis vedoucí(ho) ústavu/katedry

  
prof. Ing. Michael Valášek, DrSc.  
podpis děkana(ky)

## III. PŘEVZETÍ ZADÁNÍ

Student bere na vědomí, že je povinen vypracovat bakalářskou práci samostatně, bez cizí pomoci, s výjimkou poskytnutých konzultací. Seznam použité literatury, jiných pramenů a jmen konzultantů je třeba uvést v bakalářské práci.

28.4.2021  
Datum převzetí zadání

  
Podpis studenta

## Prohlášení

Prohlašuji, že jsem tuto práci vypracoval samostatně, a to výhradně s použitím pramenů a literatury, uvedených v seznamu citovaných zdrojů.

V Praze dne: .....

Podpis .....

## Anotace

Cílem této práce je identifikace materiálů vhodných pro tvorbu nového typu implantátů s nižším elastickým modulem a depozice funkčních vrstev titanu na tento substrát. Vlastní depozice je provedena novou technologií studené kinetizace (cold spray, CS) v rámci mezinárodní spolupráce s Politecnico di Milano, Itálie. Dalším cílem práce je charakterizace zhotovených vzorků a diskuse jejich vhodnosti vzhledem k zamýšlené aplikaci.

## Klíčová slova

Náhrady pevných tkání, biomateriály, žárové nanášení, technologie cold spray

## Annotation

The task of this bachelor thesis is to identify materials suitable for a new generation of implants with a lower elastic modulus and a deposition of functional layers of titanium on this substrate. The actual deposition is performed by a new technology of cold kinetization (cold spray, CS) within the international cooperation with Politecnico di Milano in Italy. Another goal of this thesis is to analyze the samples and discuss their suitability with respect to the intended application.

## Keywords

Hard tissue replacements, biomaterials, thermal spraying, cold spray technology



## Poděkování

Děkuji především vedoucímu mé bakalářské práce Ing. Janu Čížkovi Ph.D. za trpělivý a odborný přístup. Dále děkuji kolegům z Politecnico di Milano (prof. Sara Bagherifard, prof. Mario Guagliano) za provedení depozice vrstvy. Také bych rád poděkoval doc. Ing. Janě Sobotové Ph.D. za možnost spolupráce s Akademií věd České Republiky a Ing. Jakubovi Klečkovi za pomoc s přípravou vzorků.

# Contents

<b>1</b>	<b>INTRODUCTION .....</b>	<b>7</b>
<b>2</b>	<b>LITERATURE REVIEW.....</b>	<b>8</b>
2.1	COLD SPRAY.....	8
2.1.1	<i>History of cold spray technology.....</i>	<i>8</i>
2.1.2	<i>Coating formation and structure .....</i>	<i>8</i>
2.1.3	<i>CS system components and their function in the deposition process .....</i>	<i>10</i>
2.1.4	<i>Process parameters.....</i>	<i>12</i>
2.1.5	<i>Cold spray versus thermal spray .....</i>	<i>13</i>
2.1.6	<i>Applications of cold spray .....</i>	<i>15</i>
2.2	BIOMATERIALS AND THEIR APPLICATIONS IN HARD-TISSUE REPLACEMENTS.....	16
2.2.1	<i>Metallic materials .....</i>	<i>16</i>
2.2.2	<i>Ceramic materials .....</i>	<i>17</i>
2.2.3	<i>Polymers.....</i>	<i>18</i>
2.3	COLD SPRAY AND HARD-TISSUE IMPLANTS.....	18
<b>3</b>	<b>EXPERIMENTAL SETUP .....</b>	<b>20</b>
3.1	MATERIALS.....	20
3.1.1	<i>Substrate.....</i>	<i>20</i>
3.1.2	<i>Powder .....</i>	<i>21</i>
3.2	COATING DEPOSITION AND ANALYSIS .....	23
3.2.1	<i>Deposition parameters.....</i>	<i>23</i>
3.2.2	<i>Specimen preparation process.....</i>	<i>23</i>
3.3	ANALYSIS METHODS .....	24
<b>4</b>	<b>RESULTS AND DISCUSSION .....</b>	<b>27</b>
4.1	RESULTS .....	27
4.1.1	<i>Microstructure .....</i>	<i>27</i>
4.1.2	<i>Chemical composition .....</i>	<i>30</i>
4.1.3	<i>Phase composition .....</i>	<i>33</i>
4.2	DISCUSSION.....	34
<b>5</b>	<b>CONCLUSION .....</b>	<b>36</b>
<b>6</b>	<b>LIST OF FIGURES .....</b>	<b>37</b>
<b>7</b>	<b>REFERENCES .....</b>	<b>38</b>

# 1 Introduction

Throughout the recent history, the need to increase the reliability of hard tissue replacements has led to development and use of different metallic materials, ranging from ferrous, to cobalt-chromium-based, to titanium-based. Unfortunately, all of these exhibit relatively high elastic moduli, significantly higher than that of human bones. Upon implantation, this may lead to several undesired phenomena and, eventually, even to the implant failure.

This fact calls for the need to develop a new generation of implants that use alloys with low elastic modulus. Needless to say, this presents another challenge since such alloys (e.g. magnesium alloys are very attractive in this regard) usually do not show full biocompatibility. During interaction with human body, these are highly susceptible to corrosion and in fact even release harmful elements. Should these alloys be used, it may be necessary to protect/shield their surfaces from the corrosive environment of the human body with a bioactive layer.

The theoretical part of this work summarizes the basic knowledge about cold spray technology and the issue of biocompatibility of solid tissue replacements. A suitable combination of substrate and powder materials to form a bioactive layer is selected: AZ31 and Ti, respectively. In the experimental part, the coating is deposited onto the substrate using cold spray technology, and subsequent analysis and evaluation of their properties is presented.

The results of this first trial show there is a potential in applying of cold spray technology for the bioactive coatings on mechanically and thermally sensitive substrates. The research will therefore further continue to more advanced bioactive materials.

## 2 Literature review

### 2.1 Cold spray

#### 2.1.1 History of cold spray technology

The first recorded patent of applying a metal coating upon a substrate dates back to 1902, when Thurston invented a method, where metal particles are accelerated against a metal plate by a blast of pressurized gas with enough force so that the particles become embedded in the surface of the metal and function as a permanent coating.

However, it was not until 1980s when a proper technology of depositing non-melted particles called cold spray (CS), supersonic particle deposition (SPD), kinetic metallization (KM) or cold gas dynamic spraying (CGDS) was invented in Russia by professor Anatolij Papyrin and his group of scientists and researchers [1].

Currently, cold spray is a reliable and broadly used coating technology that can be readily purchased as a turn-key solution. It is capable of producing ultra-thick deposits that serve as either protective or performance enhancing layers, near net shapes and even freeforms [2].

#### 2.1.2 Coating formation and structure

Cold spraying is a coating technique based on depositing solid-state particles onto a substrate using a very high velocity gas flow. Powder particles with a typical diameter of 5-50  $\mu\text{m}$  are carried through a de Laval nozzle where they attain enough velocity to plastically deform upon impact with the substrate material and produce a continuous and dense coating with a wide range of thicknesses and deposition rates up to 14 kg/h [1].

The bonding of materials in cold spraying is based on the deposited particle interacting with the substrate in a solid state through plastic deformation. Such interaction usually comprises three different phenomena. First, metallurgical bonding, i.e., a diffusive bonding between the two metals in contact. Second, mechanical interlocking, i.e., a formation of localized coating material extrusions into the substrate (or vice-versa), forming a mechanical trap. The final mechanism called mechanical intertwining is a mechanism similar to interlocking, but with a higher degree of entanglement between the substrate and the coating [3]. All of these mechanisms contribute to the strong bonding between various coating-substrate combinations [4] [5] Figure 2.1 illustrates the stages of the coating formation process [2].

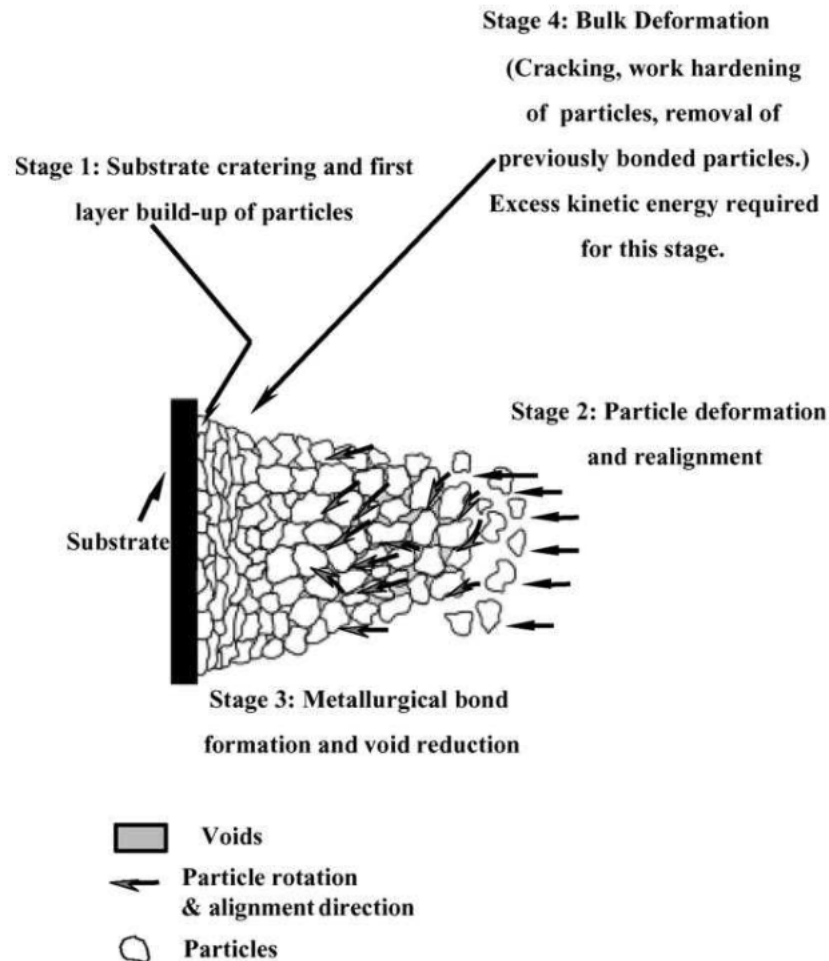


Figure 2.1. Cold spray coating build-up process [1]

Prior to the spraying, the surface of the substrate material may go through a preparation process consisting of degreasing or chemical cleaning. In special cases, grit blasting of the surface is also employed [6].

In the subsequent deposition process, the first layer of particles deforms the substrate's surface. After the first thin layer of particles is deposited, the dislocation density in the coating material rises, which increases the strength and hardness. Several factors play a part in the deformation magnitude, such as the substrate-particle interaction, or the particles' in-flight velocity and temperature [7].

A mathematical model by Bae et al. [2] depicts particle-substrate interactions in context with the hardness of the substrate and the spray particles. The variety of particle-substrate interactions on the interface are shown in Figure 2.2 [2].

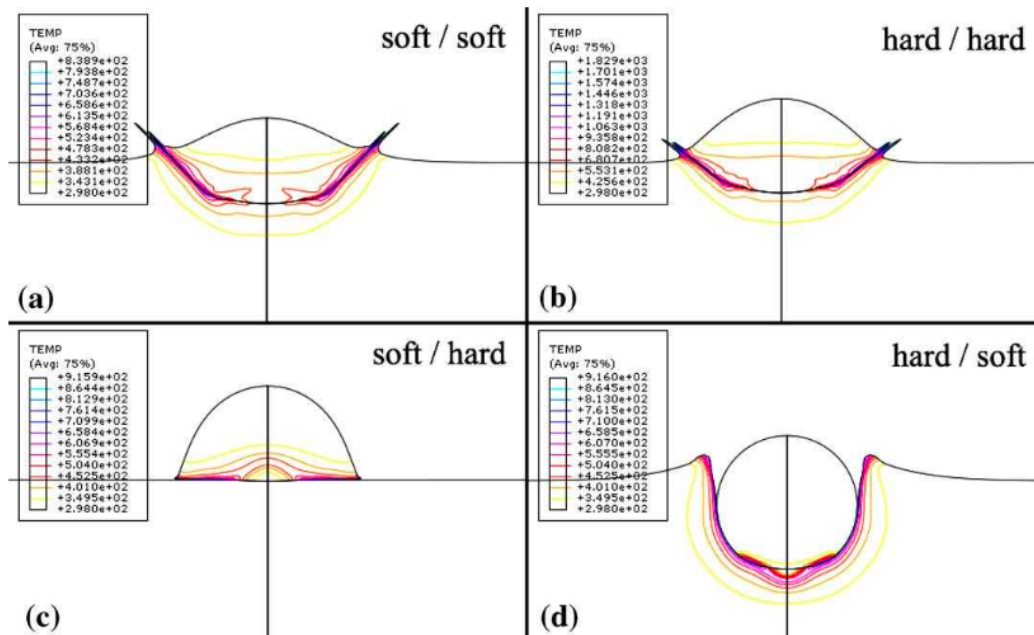


Figure 2.2. Particle-substrate interactions [6]

The next stage of a CS coating build-up consists of particle deformation and realignment caused by successive collisions of particles. Metallurgical bonds are formed between the particles in the third stage of the process, with decreasing porosity thanks to the hammering effect [7]. The final cold sprayed coating displays a dense, deformed structure with exceptional adherence and low porosity.

### 2.1.3 CS system components and their function in the deposition process

A conventional cold spray system consists of a prechamber, a converging-diverging supersonic nozzle, a powder feeder, a gas heater, a source of compressed gas, a spray chamber and a control unit which monitors and adjusts spray parameters. Figure 2.3 depicts a typical CS setup.

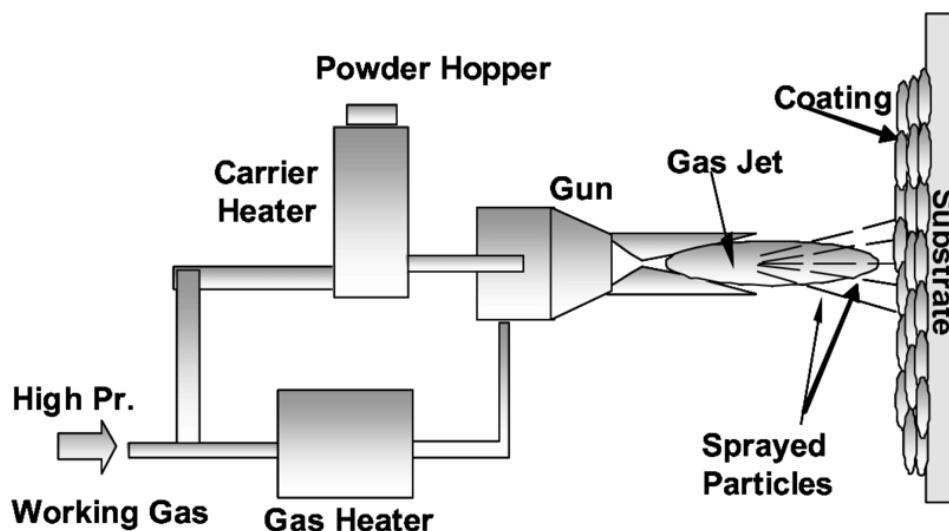


Figure 2.3. A typical cold spray setup [8]

The deposition process itself begins with highly pressurized nitrogen, helium, their mixture, or even dry air supplied into the gas preheaters through a regulator which controls the pressure. The high-pressure gas is then heated in the main preheater section and exits through the final nozzle. At the same time, less pressurized gas used for carrying the powder particles is led through a powder feeder and an optional carrier gas preheater into the nozzle by another inlet. Together with the high-pressure gas, the converging-diverging nozzle (de Laval type) aids in accelerating the powder particles to high velocities [8]. As the gases and the powder pass through the converging part of the nozzle, they are subject to a rapid compression, yielding a velocity gain. The gas + particle mixture then accelerates even more in the diverging part of the nozzle, where the velocity of the particles reaches its peak values ranging from 300 m/s up to 1200 m/s. A typical cold spray gun with a de Laval-type nozzle is pictured in Figure 2.4 [6].

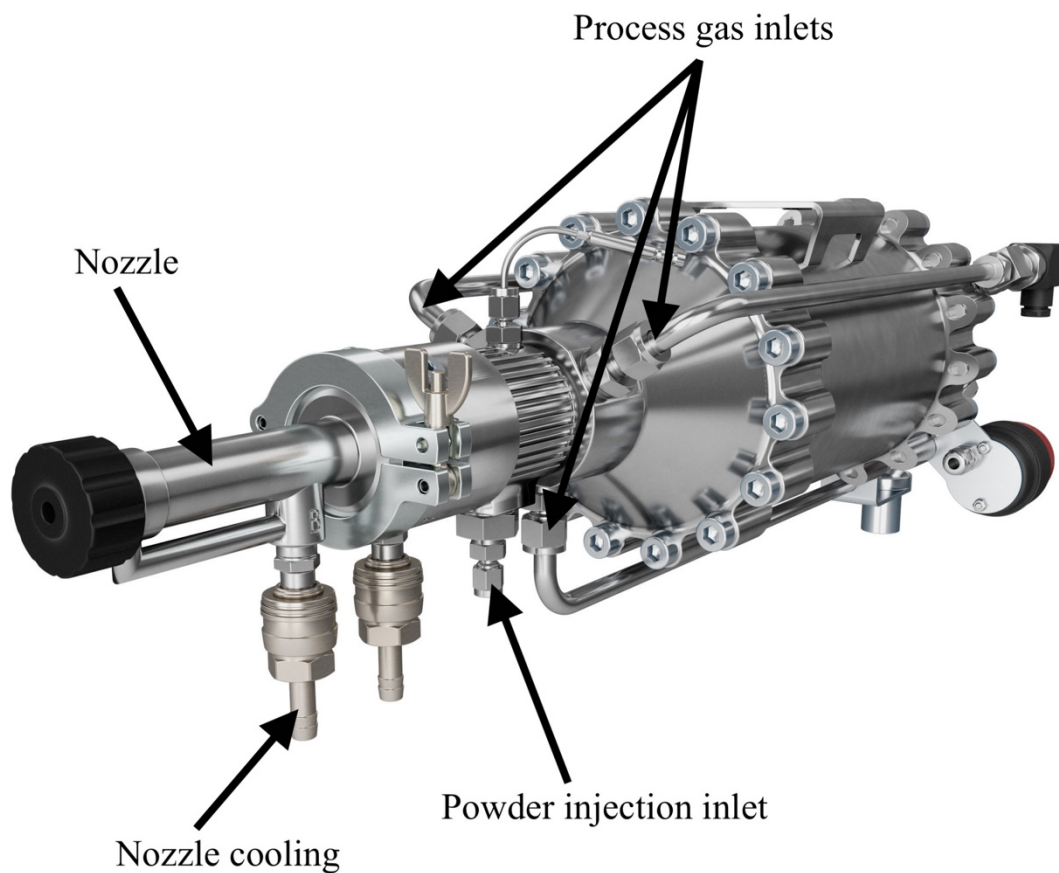


Figure 2.4 A commercial CS gun [9]. Courtesy of Impact Innovations, GmbH., Germany.

## 2.1.4 Process parameters

The cold spray process and the respective coating formation were explained in the previous sections. The process parameters tie them with each other. In CS, kinetic energy of the particles is the most important factor, and its magnitude is influenced by several parameters, such as the gas temperature and pressure, the type of propellant gas and the nozzle design, or the size and morphology of the feedstock particles. Among other, the kinetic energy increases with decreasing density and particle size. On the other hand, too light or small particles are pronouncedly affected by another phenomenon called bow shock. The bow shock wave is generated as the sprayed particles come into the close vicinity of the substrate where the surrounding gas molecules rapidly decelerate before impacting the surface. As a result, a stagnant zone emerges on the particle-substrate interface and slows down the oncoming particles. Under such conditions, the lighter and smaller particles are difficult to be deposited [8] [10].

As explained, the particle kinetic energy (i.e., velocity) has a major effect on the whole cold spray process. Every material needs to be sprayed above a threshold value, the so-called critical velocity. When the velocity does not reach the critical value, particles only have an abrasive effect on the surface of the substrate and are unable to form a coating. At the same time, in order to avoid erosion, the material should also be sprayed below a second threshold value, its upper limit. If the velocity is too high, materials lose their ability to attach to the substrate and erode the surface instead. The interval of the two limit values is known as the window of deposition. Equation 2.1 by Schmidt et al. [1] presents the estimate of the critical velocity for a typical 25- $\mu\text{m}$  diameter particle:

$$v_{cr} = \sqrt{\frac{A\sigma}{\rho} + Bc_p(T_m - T)}, \quad (\text{Eq. 2.1.})$$

where A, B are the fitting constants,  $\sigma$  is the flow stress,  $\rho$  is the density,  $c_p$  is the heat capacity,  $T_m$  the melting temperature and T is the average in-flight temperature of the particle. Figure 2.5 shows a deposition window for a selection of most commonly cold sprayed metallic materials. It is important to add that the graph was published in 2009. In the past few years, advances in cold spray systems have made it possible even for materials such as Inconels and Ti-6Al-4V to be perfectly sprayable with gas temperatures reaching up to 1200 °C with 7 MPa of pressure. [1] [4]



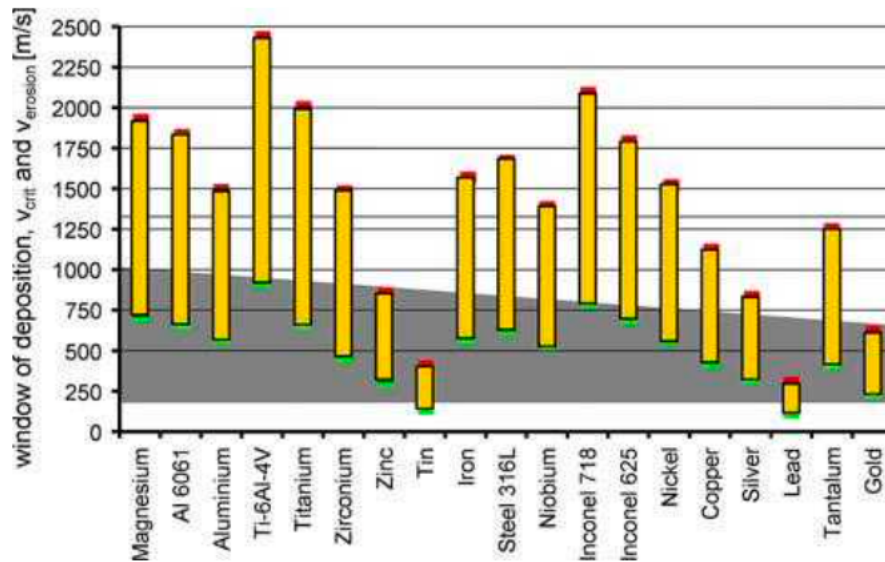


Figure 2.5. Deposition window for metallic materials, commercial cold spray systems operated inside the gray area in 2009 [8]

### 2.1.5 Cold spray versus thermal spray

The main difference between cold spraying and other thermal spray methods is the energy input: while cold spray uses heat only to pressurize the gas and thus further speed up the particles (which, nevertheless, remain in a solid state), thermal spray demands a larger energy input to heat up the particles beyond their melting point. Contrary to cold spray, particles sprayed with a thermal spray system therefore undergo a phase transformation in order to melt. This process is usually further accompanied with oxidation and residual tensile stress formation inside the coatings, often resulting in degradation of mechanical properties. Vacuum plasma spraying can eliminate these disadvantages. However, this technology is more energy and resource-consuming in comparison to cold spray.

The diagram shown in Figure 2.6 summarizes the differences between individual thermal spray technologies in terms of their in-flight particles' velocity and temperature [10]. The differences in morphology of typical single splats and microstructure of coatings sprayed by different methods are illustrated in Figures 2.7 and 2.8.

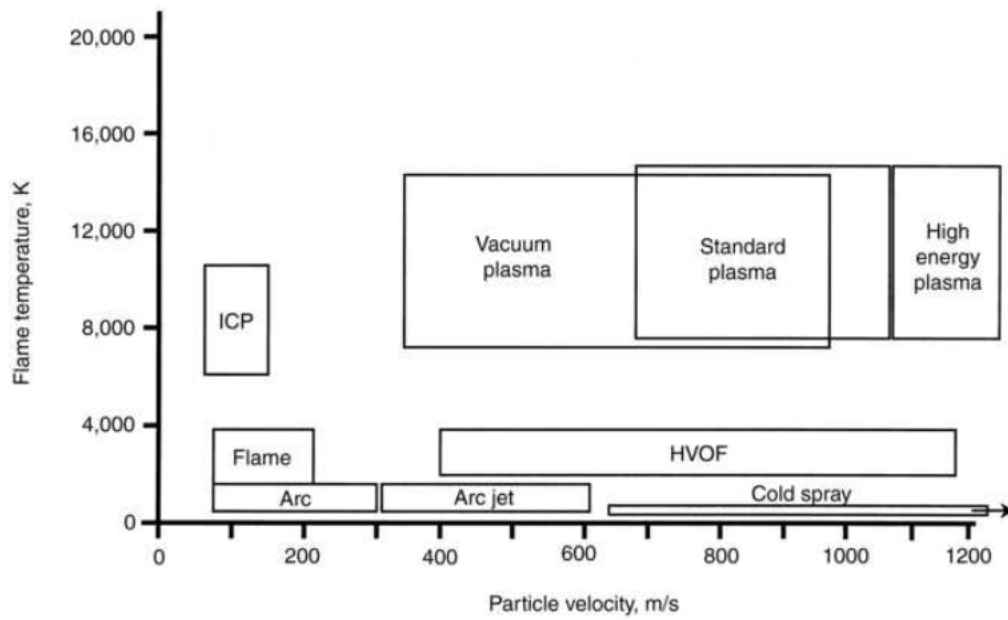


Figure 2.6 Characteristic process windows for different spraying methods [2].

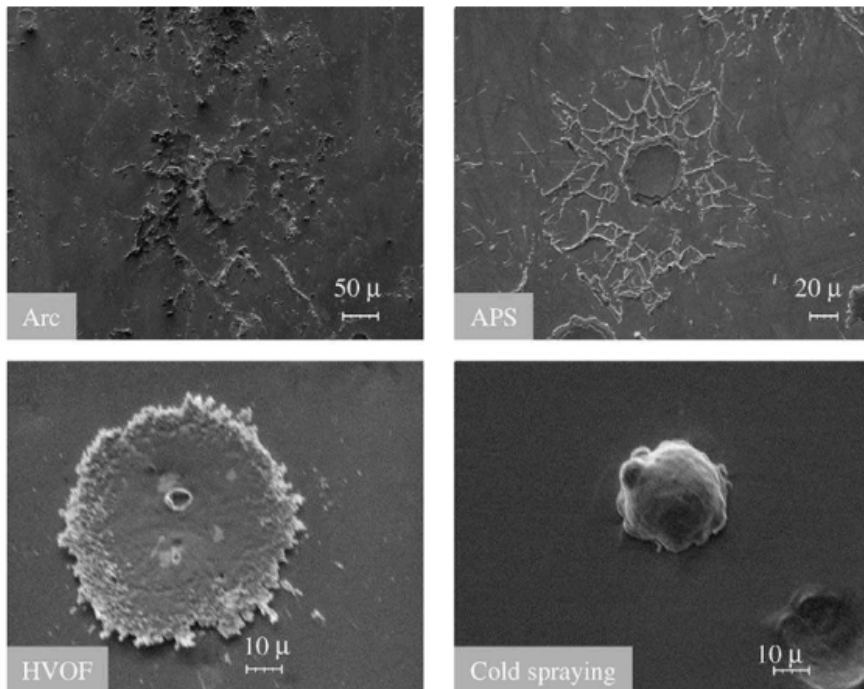


Figure 2.7 Morphologies of single splats (illustrated using Ni-5 wt.% Al) deposited by different spraying techniques [7].

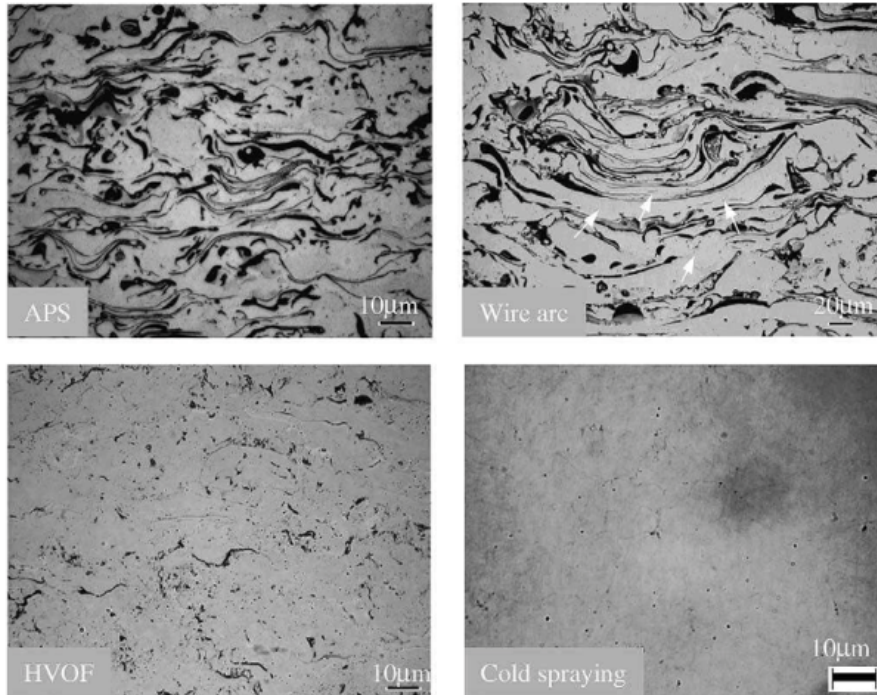


Figure 2.8 Cross-sections of average coatings (illustrated using Ni-5 wt.% Al) produced by different methods [7].

In general, thermal spray methods offer a flexibility of material selection: because of the associated high temperatures readily exceeding the melting point of most materials, the technology can be applied to a wide range of materials. The limitations here are materials that would melt or evaporate (e.g., polymer-based materials, or low melting point metals used as substrates). In contrast, cold spray offers a more narrow range of sprayable materials (mostly limited to those that can plastically deform, such as metals or mixture of ceramics and metals), but produces high purity, mechanically strong, and dense coatings [10].

### 2.1.6 Applications of cold spray

Cold spray technology offers the potential to broaden the field of applications for the entire thermal spraying sector. Cold spray is used in both production and restoration in industries such as automotive, aerospace, electronics and medical. Unlike other thermal spray processes, as a result of cold sprays high deposition rates and compressive stresses formation, another possible application is additive manufacturing [8].

In aerospace industry, cold spray is used for aluminum coatings, repairs of space shuttle rocket boosters, additively manufactured lightweight structures in airplanes, in refurbishing gas turbines or in coating magnesium alloy gearboxes used in helicopters. [9]

In electronics, cold spray is specifically used in coating aluminum tips of the electric mains with copper to protect the wires from electrochemical corrosion. CS is also able to

produce complicated conductive patterns in solar cells and to improve the surface properties of polymer-matrix composites in wind turbines. [9]

Owing to its advantages, cold spray could be potentially successfully employed in biomedicine: the prospect of producing pure, non-oxidized coatings of e.g., titanium, or even magnesium and other reactive metals and their alloys to be used as implants is alluring [9].

## 2.2 Biomaterials and their applications in hard-tissue replacements

Several decades ago, biocompatibility was only judged by the ability of a material to resist the human body environment without degrading. Because of this factor, the main goal was developing inert materials with non-allergic, non-toxic and non-carcinogenic behavior. Nowadays, this concept is considered insufficient and a positive bioactivity of a material is further required, which raises the need to coat otherwise bioinert implants with bioactive coatings that help accelerate the process of healing and raise the chances of a body accepting the implant successfully. [11]

The task of replacing/restoring bones comes with several difficulties for both endogenous or exogenous bone tissues. Endogenous substances are of limited quantity and require the patient to undergo an additional surgery. Exogenous implants have a danger of transmitting disease or being rejected by the organism and are overall inferior in terms of biocompatibility to the endogenous material. To compensate for this, in case of artificial materials, it is necessary to produce hard tissue replacement implants which mimic a natural human bone both structurally and chemically. [11]

### 2.2.1 Metallic materials

Biocompatible metallic materials have been widely used for hard tissue implants and replacements mainly because of their excellent mechanical properties and mechanical performance reliability. Despite these major advantages, metallic biomaterials come with few downsides, such as the reactivity of the involved (alloying) elements and their interaction with cells surrounding the implant. The second downside is the somewhat limited bioactivity of most metals. In prosthetic applications, materials such as ferrous alloys (austenitic stainless steel 316L, Fe-Mn), magnesium alloys (Mg-6Zn, AZ51, AZ91), titanium alloys (Ti-6Al-4V, Ti-6Al-7Nb), cobalt-chromium alloys (Co-28Cr-6Mo, Co-20Cr-15W) are broadly applied [6]. Table 2.1 shows mechanical properties of essential metallic biomaterials in comparison with human cortical bone. [12]

316L, an austenitic stainless steel, is a widely used alloy in bone replacements. However, its Young's modulus and tensile strength are about ten times higher than those of a human bone. This fact introduces a few problems, mainly the stress shielding effect, which prevents the surrounding tissue from carrying enough load, leading to bone cells extinction and the implant failure. Another downside is cytotoxicity of Cr- and Ni-ions. [12]

Co-28Cr-6Mo is another alloy with a wide field of use. Compared to 316L, CoCrMo shows a better corrosion and wear resistance, but concerns about biocompatibility and mechanical properties are almost the same as with stainless steel

Compared to stainless steel and CoCr alloys, titanium alloys show more bone-like mechanical properties, mainly a lower Young's modulus, high fatigue strength and good corrosion resistance. The main problem with titanium alloys is their low wear resistance, which is problematic in load-bearing articular implants, where abrasive wear is unavoidable. However, titanium alloys display the most sympathetic response from the surrounding tissue, which leads to research on how to improve the wear resistance using cold spray or thermal spray. Currently, the most used alloys are Ti-6Al-4V, Ti-6Al-7Nb and Ti-5Al-2.5Fe, but due to the toxicity of elements such as Al and V, newer alloys such as Ti-45Nb, Ti-30Ta and Ti-29Nb-13Ta-4.6Zr are recognized as more suitable for implant materials [12].

Table 1 Selected mechanical properties of metallic biomaterials a human cortical bone [1]

Material	Young's modulus	Tensile strength	Fracture toughness	Compressive strength	Hardness	Density
	GPa	Mpa	Mpa m <sup>1/2</sup>	MPa	HV	g/cm <sup>3</sup>
Bone	12 - 21	60 - 130	3 - 6	130 - 180		1,3 - 2,1
AISI 316L	190	930 - 1350	50 - 200	170 - 310	150 - 190	8
Ti6Al4V	110	900 - 1200	55 - 115	758 - 1117	350	4,4
Co28Cr6Mo	210	650 - 1600		450 - 1000	270 - 350	8,3
Ti30Nb/Ti30Ta	60 - 80	700 - 750				
Mg	41 - 45	230	15 - 40	65 - 100		1,7 - 2,0
α-Al <sub>2</sub> O <sub>3</sub>	400	200-300	4 - 5	4250	2400	3,96

## 2.2.2 Ceramic materials

The main difference between ceramics and metals is their bond. While metals and metal alloys display ductile and tough behavior owing to their metallic bond, ceramics tend to be very hard and brittle due to the covalent bonding. That said, despite the superior biocompatibility of ceramics over the metals, it is not possible to produce hard tissue



implants made solely of ceramics at the moment. Instead, the solution of a metallic core coated with biocompatible ceramics is used [13].

Because of its structural analogy to natural bone, hydroxylapatite (HA) has become a widely used biomaterial for its excellent biocompatible and bioactive properties. HA coatings have been successfully deposited using thermal spray processes for years, mainly with plasma spraying. However, cold sprayed HA coatings are already in the experimental stage. For example, Noorakma et al. [7] have validated the deposition of HA coatings by cold spraying onto various substrates. [13]

Bioactive glass is a type of materials with diverse compositions which allow a steady bonding with the surrounding living tissue. In the past few years, there have been attempts by Bolelli et al. to deposit a bioactive glass coating of composition  $K_2O-CaO-P_2O_5-SiO_2$  using high velocity suspension technique. [13]

### 2.2.3 Polymers

The reason for substituting hard tissue with a polymeric implant is to more closely mimic mechanical properties of the natural bone, in particular its relatively low elastic modulus. However, polymers are perceived only as a marginal group in terms of thermal spraying due to the difficulty in optimizing spray parameters because of detrimental transformations triggered by the heat. It seems that cold spray technology can overcome these limitations by depositing particles beneath the critical temperature [14].

PEEK is broadly used for hard tissue implants, mainly intervertebral disk replacements because of its chemical stability, good mechanical properties and a reduction in MRI artefacts in comparison to metallic biomaterials. The downside of using PEEK as a bio-implant material is its inert behavior and its inability to bond intimately with the surrounding tissue [14].

Also known as nylon, polyamide is a broadly used material in medical devices. Two types of polyamides, PA6 and PA66, are being reinforced with glass fibers to gain better mechanical properties. However, polyamide tends to have hydrolytic behavior and absorbs water very well, which results in a deterioration of mechanical properties [14].

## 2.3 Cold spray and hard-tissue implants

Because of their high plasticity and ability to effectively produce high quality coatings, bioactive metals (stainless steel and titanium) were the first ones to be sprayed with CS. In case of titanium, analogically to the porous structure of plasma-sprayed coatings, cold-spray is also able to produce these with the aim to allow bone ingrowth. Last, cold sprayed coatings also completely isolate the substrate material from the corrosive human body

environment and, by doing so, prevent any potential toxic particles from dissolving into the body from the substrate [12].

The latter opens up a pathway to applying cold sprayed biocompatible or even bioactive coatings to lower or even non-biocompatible substrate materials, but whose mechanical properties (e.g., Young's modulus) are closer to those of a human bone when compared to steels or CoCr-based materials. In particular, this holds true for magnesium and magnesium-based alloys, i.e., alloys with too low melting points for high temperature thermal spray methods. In fact, first studies already appeared: cold sprayed HA coating on a magnesium alloy (AZ51) substrate has been successfully applied by Noorakma et al. [7].

Nevertheless, as of now, cold sprayed titanium alloys coatings on magnesium have not been studied. The primary aim of this study is to investigate the possibility to deposit functional Ti-based coating onto a selected low-modulus magnesium alloy, an essential step in an effort to widen the CS potential for bioapplications.

### 3 Experimental setup

This chapter will describe the materials used in the experimental part of this thesis, as well as the procedure of cold spray deposition of the coating. Last, the analytical methods used to characterize the produced samples will be provided in more detail.

#### 3.1 Materials

##### 3.1.1 Substrate

The substrate of choice was a rectangular  $100 \times 100 \text{ mm}^2$  specimen made of cold-rolled and annealed AZ31 Mg-alloy with a thickness of 6 mm, supplied by Alfa Aesar, GmbH. (Germany). Prior to deposition, the surface of the sample was grit blasted with spherical glass particles with typical sizes of 200-300  $\mu\text{m}$ . This was followed by ultrasonic cleaning, realized in ethanol to prevent excessive oxidation.

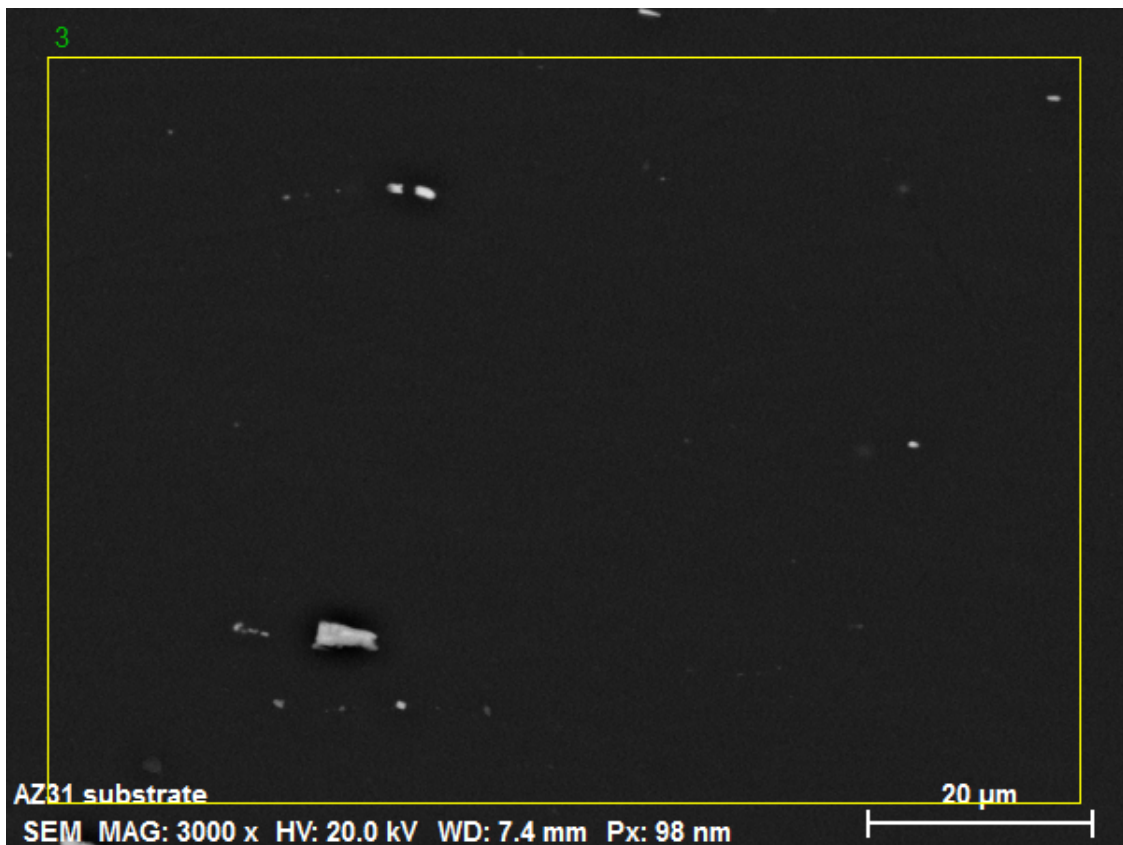


Figure 3.1 Substrate elemental mapping



Table 2: AZ31 substrate chemical composition

Element	Wt. %
Mg	95,4
Al	2,7
Mn	0,2
Zn	1,3
O	0,4

Chemical analysis of the substrate was determined using EDX (Figure 3.1, Table 2). The chemical composition we measured matches the nominal composition of an AZ31 alloy. A more precise distribution of elements in the substrate is further discussed in the results of EDX mapping in section 4.1.2.

### 3.1.2 Powder

Due to titanium's biocompatibility with the human body, titanium-based powders are widely employed in the medical profession for a variety of purposes. As an ISO 13485 certified supplier, AP&C (Boisbriand, Canada) provided the powder for our experiment.

Specifically, pure titanium powder with average particle sizes of 15-45  $\mu\text{m}$  was selected for this experiment. This is a particle size range smaller than what is typically used in high temperature thermal spray process, but works well for a high-pressure cold spray process. XRD analysis (Figure 3.2 confirmed its content as 100% alpha phase, with an average crystallite size of 191,670 nm and 0,053% strain. As shown in Figure 3.3, this powder is characterized by its regular, spherical morphology, which is a consequence of the technology of its production (gas atomization). Again, this spherical particle morphology that is ideal for cold spray technology.

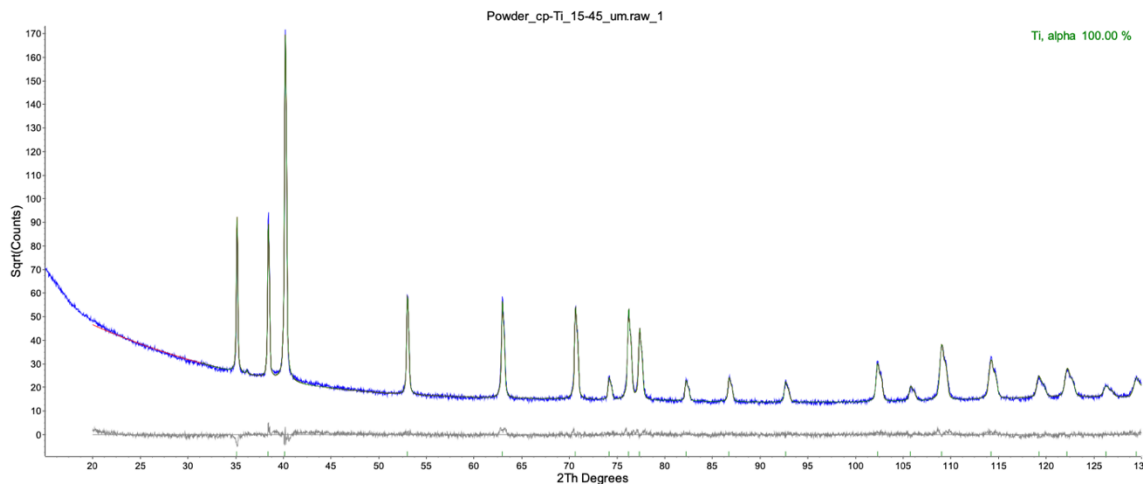
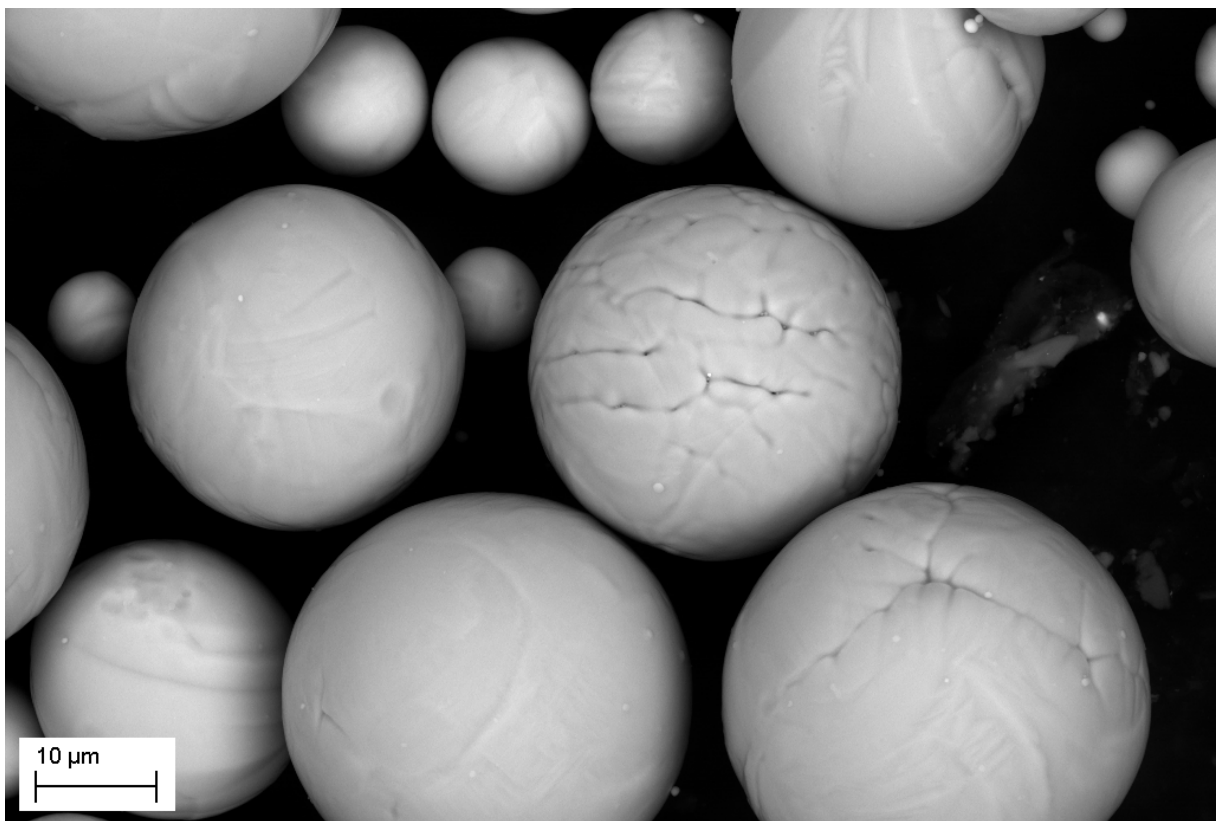
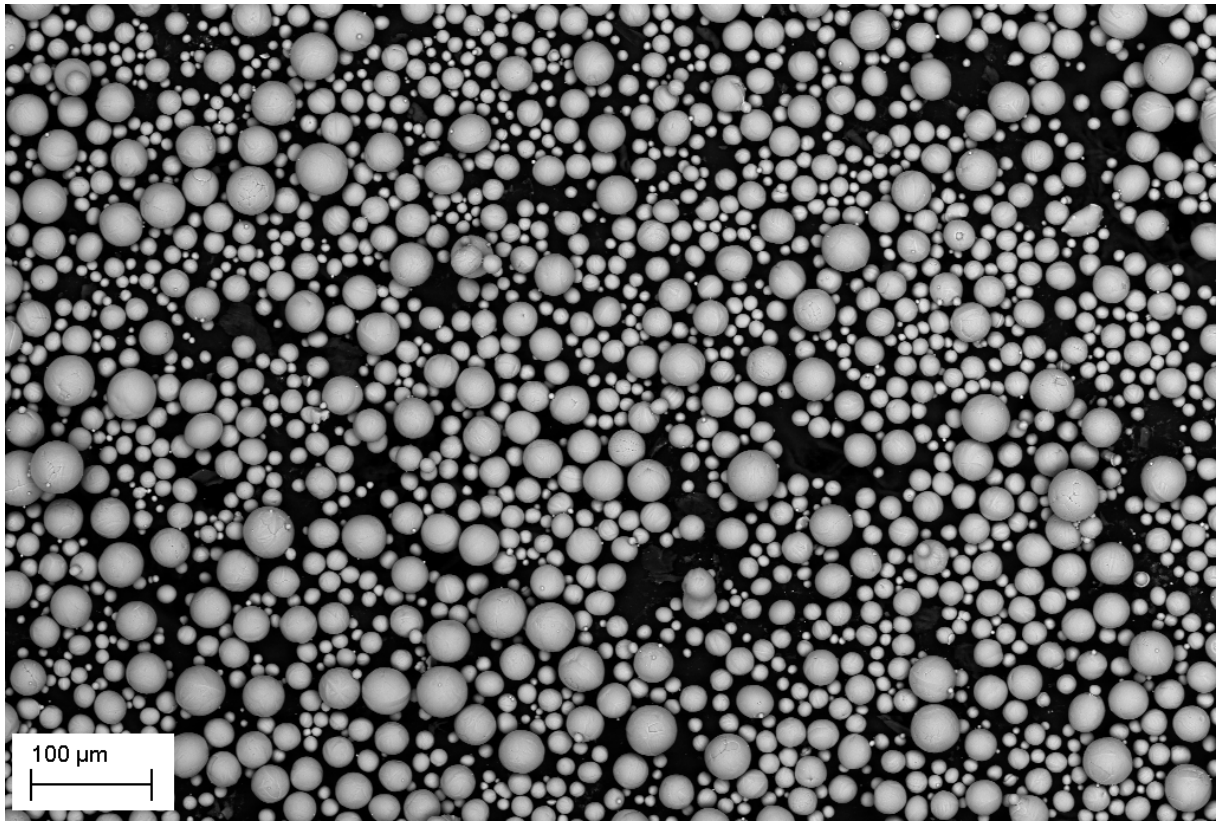


Figure 3.2 XRD analysis of the feedstock Ti powder.



*Figure 3.3 Ti feedstock powder morphology*

## 3.2 Coating deposition and analysis

### 3.2.1 Deposition parameters

Cold spray deposition of the Ti coating onto the AZ31 substrate was performed in our partner laboratory in Italy (Politecnico di Milano). For that, high-pressure cold spray system 5/8 from Impact Innovations, GmbH. (Germany) was used.

The system maximum limits are 50 bar gas pressure and 800 °C gas temperature. For this deposition, the gas pressure and temperature were set to 35 bar and 700 °C, respectively (Table 3). The stand-off distance (distance from the torch nozzle exit to the substrate surface) was set to 25 mm. Such short distances are typically used in cold spraying to prevent reduction of the particles' in-flight velocity caused by interaction with atmosphere.

Table 3: Coating parameters

<b>Deposition parameters</b>	
Gas temperature [°C]	700
Gas pressure [bar]	35
Work and carrier gas	Nitrogen
Stand-off distance [mm]	25
Powder feed rate [g/min]	15,1
Scanning speed [mm/s]	300

To comprehend development of the microstructure with thickness, four torch nozzle passes were made over the substrate surface. Given the high deposition efficiency of cold spray, this would naturally yield excessive thickness of the coating (as compared to the 100-300 µm required for the application). However, the excessive thickness would allow us to easier discover any prospective development or trend in the coating, a knowledge important in this preliminary trial.

### 3.2.2 Specimen preparation process

The produced coating was metallographically prepared for SEM and EDX observations. This involved cutting using a Struers Secotom-50 metallographic saw equipped with a diamond cutting disc and cold mounting of the samples in EpoFix resin. After the mounting, the sample was ground and polished using Tegramin-25 device and SiC papers of FEPA 220 to 4000 grain sizes, followed by a finer polishing using a composite disc

and a 9  $\mu\text{m}$  diamond paste. Further polishing was performed first with a “Dur” disc, a 3- $\mu\text{m}$  diamond suspension and a special non-water-based lubricant to prevent corrosion of the Mg alloy. After that, the specimen was further polished using “Nap” disc with a 1- $\mu\text{m}$  diamond paste. The final polishing was accomplished using an OP-S suspension (colloidal 0.025- $\mu\text{m}$   $\text{SiO}_2$ ) for an extended time.

### 3.3 Analysis methods

#### Scanning electron microscopy

A scanning electron microscope (SEM) is a device that uses a directed beam of high-energy electrons to image topography and qualitative composition of the observed sample and obtain other material information. To capture the surface of the specimens, the electron beam is deflected in a magnetic field and moved in a raster pattern. The interaction of the electron beam with the specimen, such as emission of secondary electrons (SE) or backscattered electrons (BSE), is observed and converted for imaging purposes. A conductive coating should be applied to nonconductive surfaces to improve the imaging quality [4]. The electron microscope used in our study was EVO MA 15 (Zeiss, Germany) depicted in Figure 3.4.

The imaging was performed in BSE mode to allow easier identification of the coating and the substrate materials, as well as highlighting the oxygen content partially present at particle rims (see section 4). Relatively short work distances of 7-8 mm were used to improve the yield.

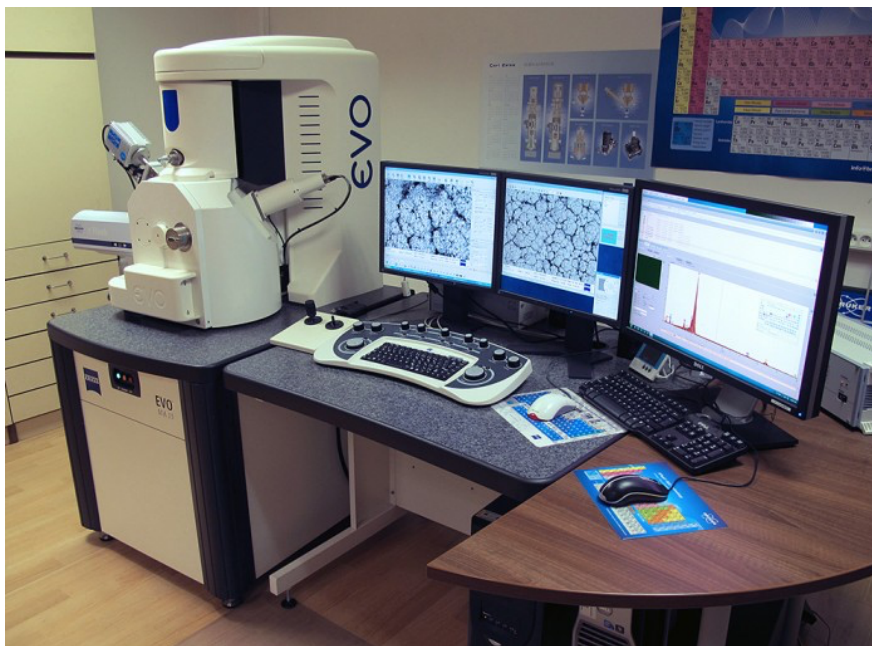


Figure 3.4 EVO MA 15 SEM used in this study.



## Porosity measurement in ImageJ

Internal porosity measurement was done using image analysis. For that, ten images at random locations in the Ti coating were captured by SEM at identical magnification. ImageJ software (NIH, USA) was then used to analyze the images. The images were converted into 8-bit depth, gray contrast and subsequently manually thresholded to differentiate the pores from the particles. The minimum and maximum threshold limits were set as 0 and 189, respectively (out of 0-255 range). The image in Figure 3.4 presents an illustration of the thresholding process.

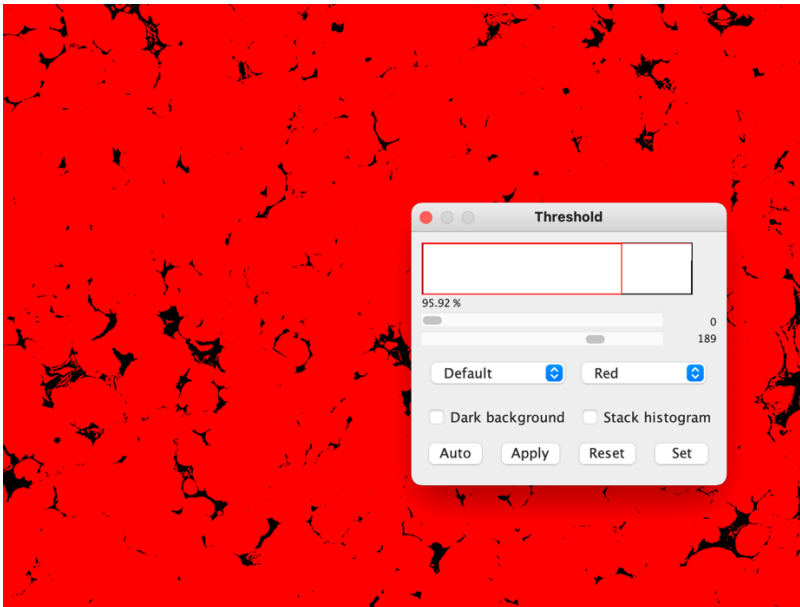


Figure 3.5 Porosity measurement in the ImageJ software, thresholding procedure.

## Chemical composition

EDX systems are commonly attachments to electron microscopy instruments such as scanning electron microscopes (SEM) or transmission electron microscopes (TEM). The data generated by EDX analysis consist of spectra showing peaks corresponding to the elements making up the true composition of the analyzed sample. Elemental mapping of the sample is also possible [4].

Area analysis of the Ti coating (as well as the AZ31 substrate) was realized at low SEM magnifications to improve the statistical reliability of the obtained data. Following that, a mapping of the elemental distribution was performed at a higher magnification in the vicinity of the coating-substrate interface. This data was collected for approximately 20 minutes.

## **Phase analysis**

The phase composition of samples was determined by X-ray diffraction (XRD) method. The measurements were carried out in a symmetrical Bragg-Brentano arrangement on vertical diffractometer Bruker D8 Discover (Bruker AXS, Germany) using Cu K $\alpha$  radiation with Ni K $\beta$  filter. The diffracted beam was detected by 1D detector LynxEye. The angular range was from 20° to 130° with a step size 0.03°.

## 4 Results and discussion

In this chapter, the results obtained by different analyses of the cold sprayed Ti coating on AZ31 substrate will be presented, along with a discussion of the results and a recommendation for subsequent work.

### 4.1 Results

#### 4.1.1 Microstructure

Microstructure of the deposited Ti coating was studied by scanning electron microscope (SEM). As shown in Figure 4.1, the microstructure resembles a typical coating deposited by thermal spray technology.

Unlike high-temperature thermally sprayed coatings such as those made by HVOF or plasma spray, the structure is well connected and, with the exception of porosity, homogeneous. Individual splats are practically indistinguishable even at high magnifications (Figure 4.1).

With only 4 passes of the torch and feeding of about 15 g/min, the coating exhibits an average thickness of 860 microns, yielding a high per-pass-thickness increase of 215  $\mu\text{m}$ .

Ten randomly selected coating cross-section images captured by SEM at 500 $\times$  magnification were analyzed for porosity in ImageJ software, with the average result being 4,2%.

*Table 4: Coating porosity analysis results*

Image	Porosity (%)
1	3,8
2	4,2
3	5,9
4	4,0
5	5,2
6	3,0
7	4,1
8	4,2
9	3,9
10	4,0
Average	4,2

Contrary to the rather unoptimized porosity, the interface between the Ti coating and the AZ31 substrate is excellent (Figure 4.1), with no signs of delamination along the entire length of the spray. This observation is in accordance with the occurrence of virtually undeformed Ti particles embedded in the AZ31 substrate, signifying mechanical interlocking, a feature typical for cold spraying onto softer substrate materials.

The surface roughness of the coating is fully comparable to the typical size of the individual sprayed Ti particles. Importantly, the surface does not contain any vertical segmentation cracks, as opposed to coatings of similar thicknesses deposited e.g. by the plasma spray process.



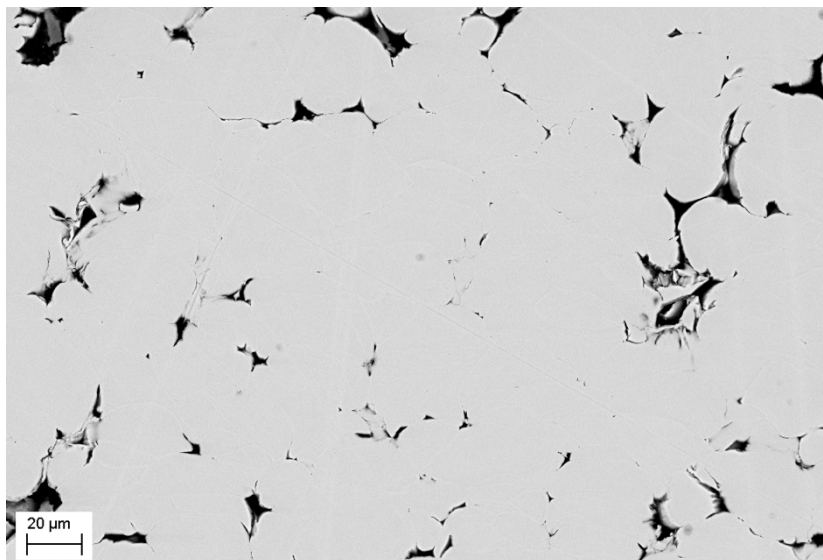
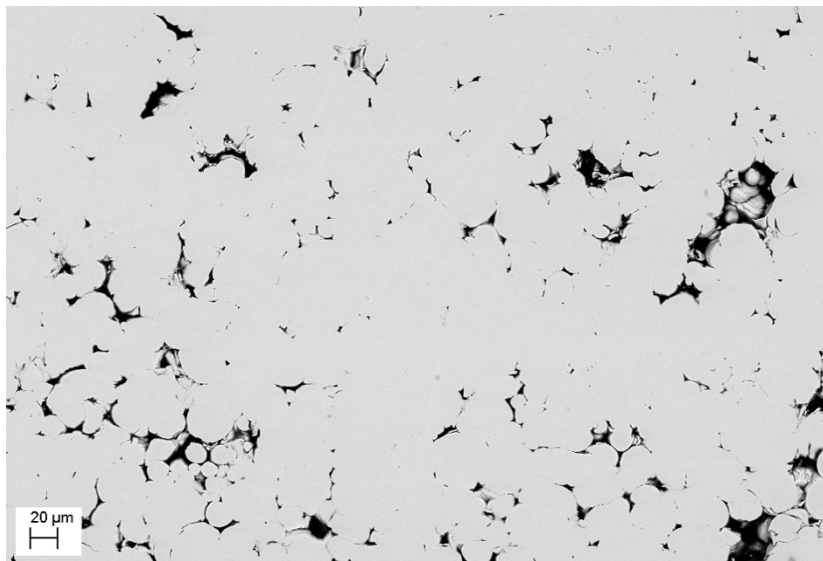
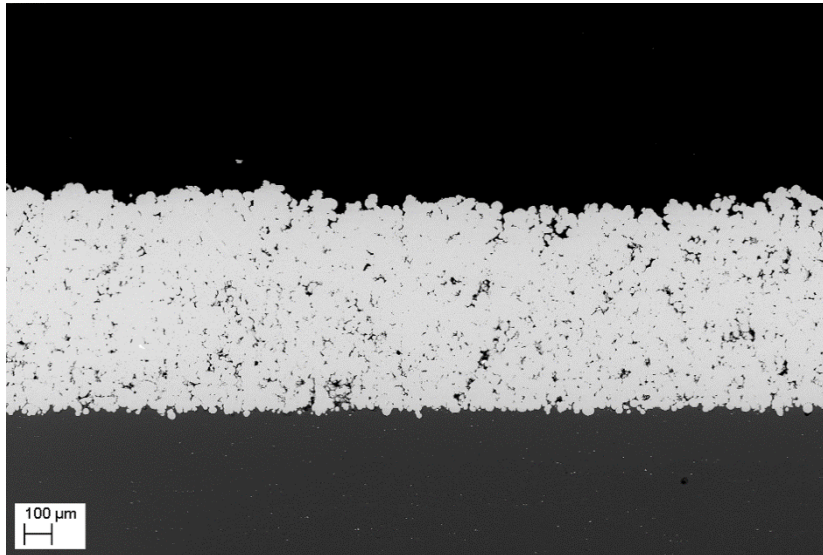


Figure 4.1 Microstructure of the cold sprayed Ti coating deposited on AZ31 substrate viewed at different magnifications. The smallest magnification allows to appreciate the surface roughness of the coatings, as well as the character of the coating-substrate interface. The higher magnifications show porosity content and morphology, as well as the connection of individual Ti particles.

### 4.1.2 Chemical composition

An EDX analysis was performed to determine the composition of both the substrate (see Chapter 3) and the deposited coating. An area analysis showed that the coating corresponds to almost 100% pure Ti with a minimal amount of oxygen. This was determined as 0.44 at.%, which is a value fully proportional to the starting feedstock powder. It should be noted that for light elements such as oxygen, the EDX analysis may partially be burdened by a measurement error, but the detected oxygen content is very low nevertheless.

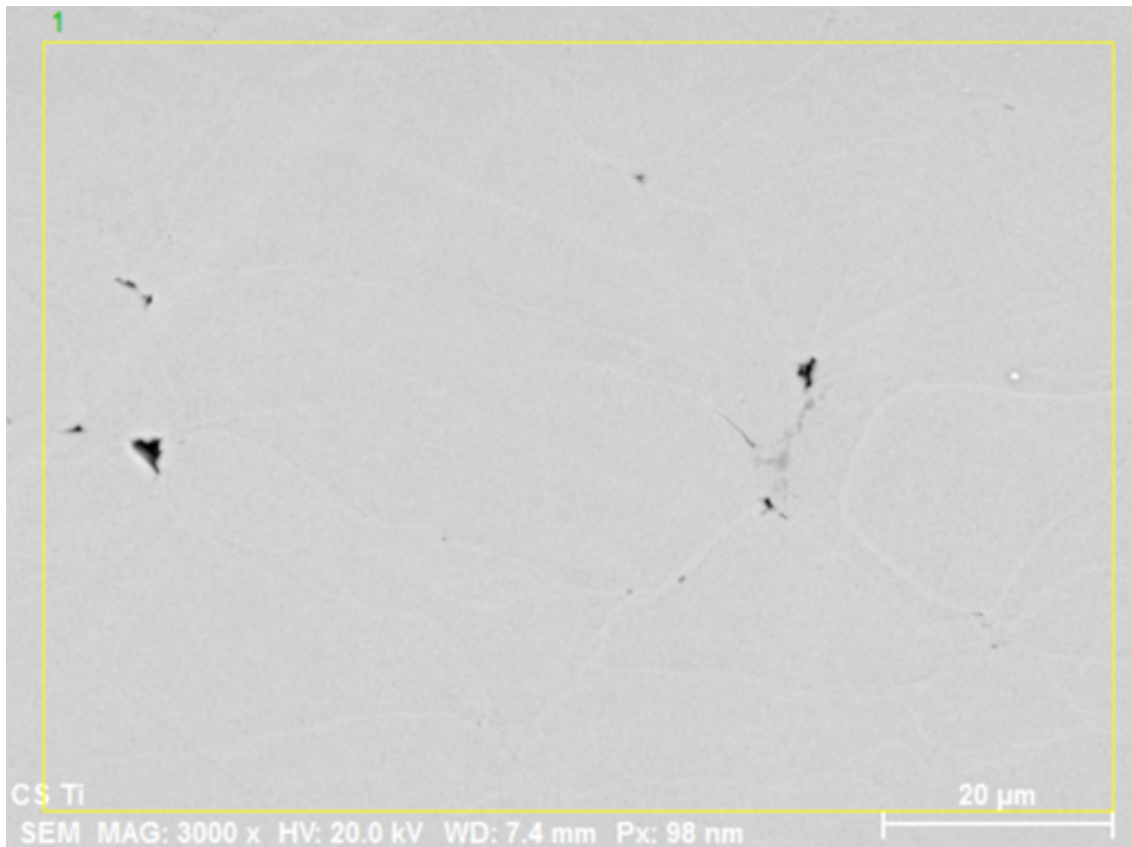


Figure 4.2 Area of the cold sprayed coating analyzed by EDX. The overall oxygen content was measured as 0.44 at.% and could be partially seen from the image as the brighter contrast lines between the individual particles, a consequence of slight oxidation of the starting feedstock powder inherited into the coating microstructure.

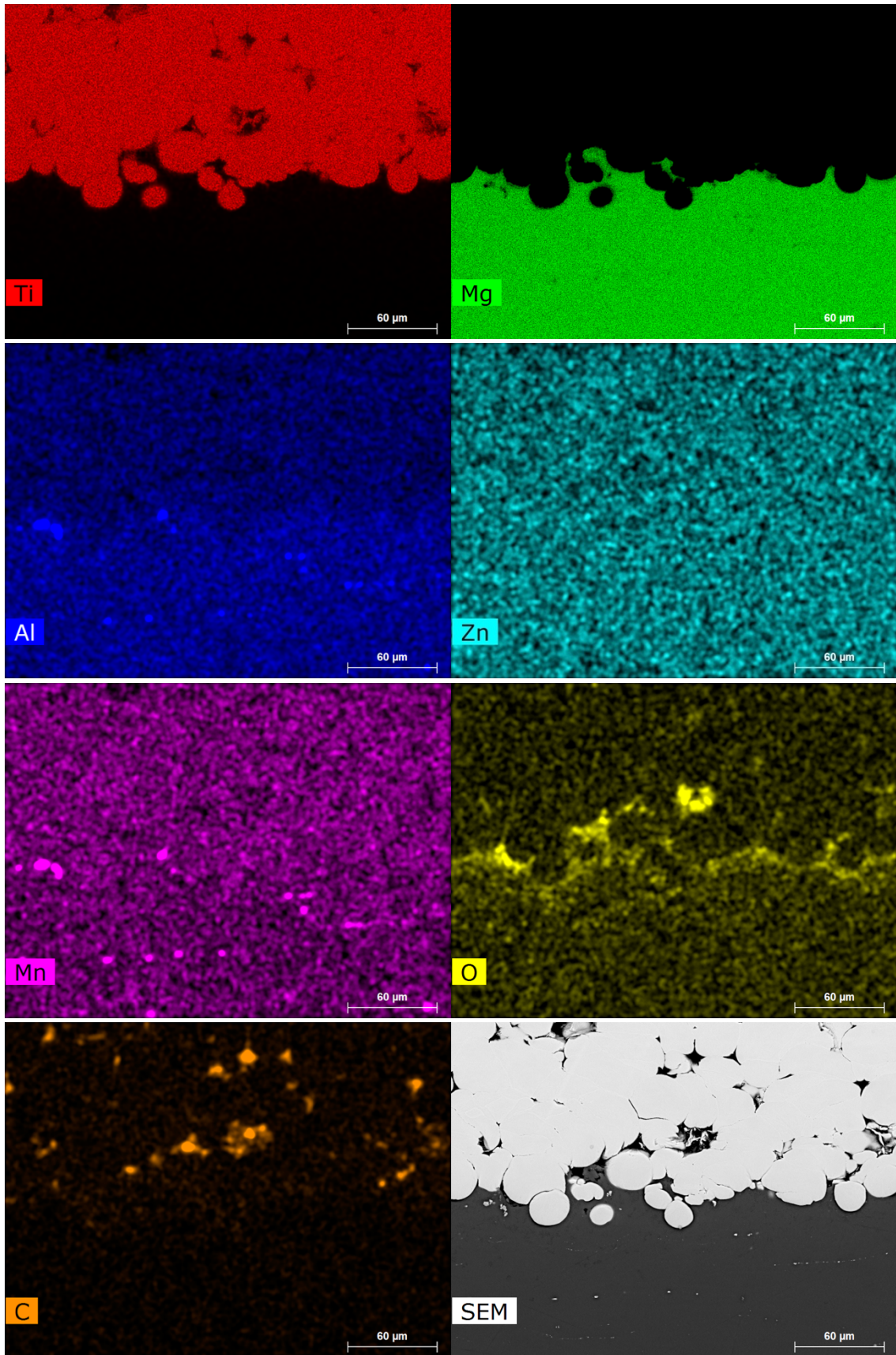


Figure 4.3 EDX mapping analysis of the coating-substrate interface region. Elements present in the coating (Ti), in the substrate (Mg, Al, Zn, Mn), and elements generally regarded as unavoidable impurities (O, C) were mapped.

Following the area analysis, an extended EDX mapping of the coating-substrate interface area was performed at a higher magnification. Based on the results, it could be claimed that titanium exclusively comprises the entire coating, while, at the same time, not being present (diffused) deeper into the substrate. Comparison of the Ti and Mg EDX maps confirms occurrence of the mechanical interlocking phenomenon described in section 4.1.1, an embedment of high-kinetic energy Ti particles into the soft AZ31 alloy.

Aluminum is the main alloying element in AZ31. Contrary to expected results, its content is not distributed homogeneously in the substrate. Instead, a slightly higher Al content is seen in precipitates present throughout the alloy. This trend is also seen for Mn content (its overall amount is very low, though, see Chapter 3) and the precipitates are obviously richer in both Al, Mn. Unlike Al, the second main alloying element, Zn, has its content distributed homogeneously throughout the alloy.

No traces of carbon are detected in the substrate, however, small regions of carbon can be seen inside the pores of the coating. The carbon content is somewhat copied by oxygen, also present mostly in the coating pores. Both readings can be partially misleading as the angled surfaces inside the pores lead to values of both elements seemingly higher than the real content. Nevertheless, slightly increased oxygen content can be also seen at the coating-substrate interface.



### 4.1.3 Phase composition

The EDX analysis suggested a minor presence of oxygen in the coatings only, a hypothesis further supported by the Ti and O<sub>2</sub> content mapping. To verify this, XRD analysis was carried out.

The results confirm that the sprayed Ti coating does not contain any other phases, except for pure titanium. At the same time, the cold spray process did not trigger any phase transformations as the Ti coating lattice was identified as 100% hcp. The sprayed particles have an average crystalline (grain) size of 73 nm, which is approximately one-third of the crystallite sizes corresponding to grains in the feedstock powder particles. The detected overall strain reached 0,086%, a value larger than in the case of the feedstock powder.

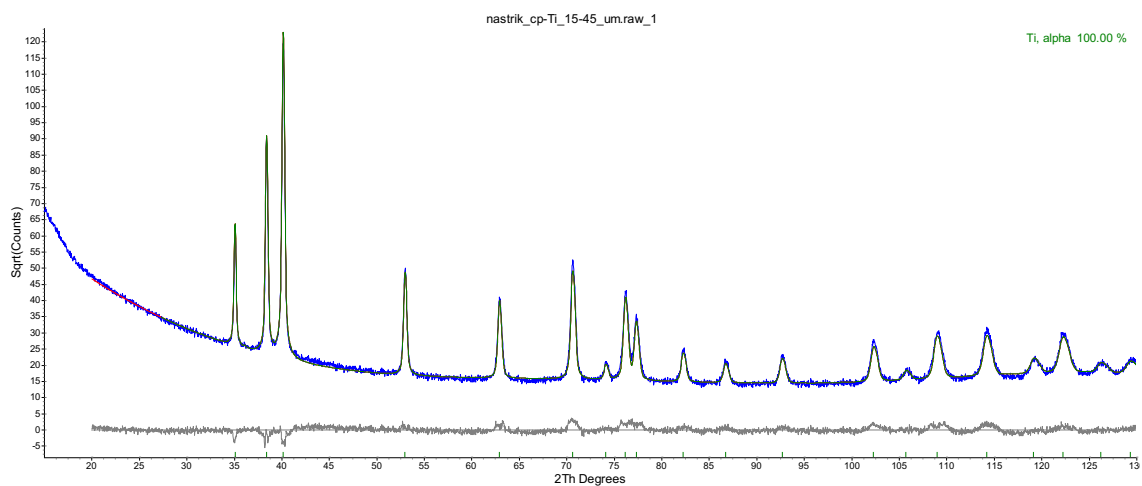


Figure 4.4 Phase analysis of the cold sprayed Ti coatings, showing 100% pure hcp titanium. The strain originating from the deposition process is manifested by slightly broader peaks toward the high detection angles.

## 4.2 Discussion

We prepared a coating consisting of pure Ti without oxidation and other undesirable changes on a substrate made of Mg alloy AZ31. The EDX mapping confirmed that almost no oxygen is present in the titanium coating. Preventing oxidation during the deposition is a characteristic property of the cold spray process and represents one of its major advantages over the generation-older high temperature processes. In these, deposition of Ti would require processing temperatures exceeding titanium melting point ( $T_m = 1680\text{ °C}$ ). Naturally, this would lead to substantial oxidation of the Ti particles, and, at the same time, would eventually melt the relatively low melting point AZ31 alloy ( $T_m = 630\text{ °C}$ ). In other words, deposition of Ti onto AZ31 may in fact not be possible by the high temperature processes at all, providing the cold spray process with a significant advantage.

Aside from the absence of oxidation during the deposition, the titanium particles also did not undergo any phase changes and the coating was identified as 100% alpha (hcp), i.e., the same as the starting feedstock. Again, the absence of phase changes in the process puts cold spray forward and presents a great promise for the future experimental work, when more complex alpha or alpha + beta coatings of Ti6Al4V or the new TiNbTaZr powder will be sprayed.

The somewhat excessive thickness of roughly 860 microns was achieved in only four torch passes. In terms of time, only few minutes spraying was needed to obtain such volume of material. This is a big advantage of cold spray process over e.g. PVD or CVD processes, where the typical maximum thicknesses reach the order of tens of microns. At the same time, no coating delamination was observed along the entire length of the sample. This indicates an excellent adhesion, caused by mechanical interlocking and metallurgical bonding between the two metals, two out of three bonding mechanisms in cold spray (the third being intermixing [5]). The first layer of particles was not virtually deformed, as opposed to a typical flattening of particles frequently observed in cold spray [15]. In the case of our study, the absence of deformation in the first layer of particles was caused by the relatively low hardness of the Mg-based substrate material. Nevertheless, cold spray is generally regarded as a technology able to deposit coatings even on soft substrates; in fact, deposition onto polymer substrates is also possible [16]. The produced coating thickness of 860  $\mu\text{m}$  is too thick for the intended application. In this case, it was deposited to allow investigation of microstructure development with increasing thickness. For the subsequent testing, it will be restricted to 150-300  $\mu\text{m}$  to better reflect the thickness optimal for potential use.

The well-connected microstructure with indistinguishable particles is characteristic of the cold spray process and presents a major difference to other thermal spray processes. In the structure, only slight contours of individual particles can be recognized, probably

because of the minor content of oxygen that follows the surfaces of the original feedstock Ti particles. Even at such thickness, the coating does not contain segmentation cracks, which typically form in coatings prepared by other deposition technologies due to quenching stresses (connected to the phase change from liquid droplets to solid splats) as well as thermal contraction after the deposition (connected to CTE mismatch of the coating and the substrate). The perfect connection of the individual particles is a basic prerequisite for the intended application, where the lower-biocompatibility metallic core of future replacements must be perfectly shielded from the environment of the human body and the corrosion effect of the body fluids. Such arrangement makes perfect use of one of the greatest advantages of CS and that is the strength of the coating-substrate bond.

At the moment, the one characteristic of the deposited Ti coating that needs improvement is the presence of pores. The porosity most likely originated due to the not ideally optimized deposition parameters in the partner laboratory (Politecnico di Milano). This was caused by the fact that the laboratory recently purchased a new cold spray system and several trials will probably be needed to fully optimize the coating properties. From the point of view of potential application, such porosity should not trigger undesirable reactions as the pores are isolated. Still, sealing of the pores is the next step in the international collaboration.

After the Ti coatings will be optimized, the next step will target more complex, Ti-based materials more suitable for bioapplications. At the moment, TiNbTaZr alloy was selected as a prime candidate and efforts to produce feedstock powder of properties suitable for cold spray deposition are already ongoing.

## 5 Conclusion

The goal of this thesis was to research the capabilities of cold spray technology in terms of depositing a bioactive coating onto a specific substrate for potential use in a new generation of hard tissue implants. In this case, AZ31 Mg-alloy was selected. The alloy exhibits lower biocompatibility levels (to be shielded by the coating), but its mechanical properties are much closer to the human bone than the currently used Ti alloys.

In chapter 2, the cold spraying process was explained alongside the cold spray system assembly and its components. Furthermore, the biocompatibility of materials, both chemical and mechanical, was discussed. In particular, this pertained to the use of bioactive coatings on substrates mechanically compatible with human bone tissue, but not chemically biocompatible on its own. Based on this research, the combination of pure titanium as a coating powder and AZ31 magnesium alloy with a low elastic modulus as a substrate was selected for the first trials.

This selection was then tested experimentally. Ti powder was sprayed onto the AZ31 substrate and the materials were subsequently analyzed. In the Ti coating, the particles were slightly deformed without signs of oxidation or other contamination. The coating did not delaminate from the substrate at any point. In terms of phase composition, the titanium powder was 100% composed of alpha phase before and after spraying. The 4.2% porosity of the coating is not optimal, but the pores are not interconnected and therefore the substrate is protected at each point by a layer of titanium.

In conclusion, it was shown that cold spray technology can be successfully used to deposit bioactive coatings onto sensitive substrates. This is an outcome that could not be achieved by high temperature thermal spray methods such as plasma spray or HVOF as the substrate material would eventually melt away and also the Ti powder would oxidize heavily. In the next step, elimination of the porosity will be attempted, followed by changing Ti for even more advanced materials, such as TiNbTaZr.



## 6 List of Figures

Figure 2.1. Cold spray coating build-up process [1] .....	9
Figure 2.2. Particle-substrate interactions [6] .....	10
Figure 2.3. A typical cold spray setup [8] .....	10
Figure 2.4 A commercial CS gun [9]. Courtesy of Impact Innovations, GmbH, Germany. ....	11
Figure 2.5. Deposition window for metallic materials, commercial cold spray systems operated inside the gray area in 2009 [8] .....	13
Figure 2.6 Characteristic process windows for different spraying methods [2]. ....	14
Figure 2.7 Morphologies of single splats (illustrated using Ni-5 wt.% Al) deposited by different spraying techniques [7].....	14
Figure 2.8 Cross-sections of average coatings (illustrated using Ni-5 wt.% Al) produced by different methods [7].....	15
Figure 3.1 Substrate elemental mapping .....	20
Figure 3.2 XRD analysis of the feedstock Ti powder.....	21
Figure 3.3 Ti feedstock powder morphology .....	22
Figure 3.4 EVO MA 15 SEM used in this study.....	24
Figure 3.5 Porosity measurement in the ImageJ software, thresholding procedure. ....	25
Figure 4.1 Microstructure of the cold sprayed Ti coating deposited on AZ31 substrate viewed at different magnifications. The smallest magnification allows to appreciate the surface roughness of the coatings, as well as the character of the coating-substrate interface. The higher magnifications show porosity content and morphology, as well as the connection of individual Ti particles.....	29
Figure 4.2 Area of the cold sprayed coating analyzed by EDX. The overall oxygen content was measured as 0.44 at.% and could be partially seen from the image as the brighter contrast lines between the individual particles, a consequence of slight oxidation of the starting feedstock powder inherited into the coating microstructure....	30
Figure 4.3 EDX mapping analysis of the coating-substrate interface region. Elements present in the coating (Ti), in the substrate (Mg, Al, Zn, Mn), and elements generally regarded as unavoidable impurities (O, C) were mapped. ....	31
Figure 4.4 Phase analysis of the cold sprayed Ti coatings, showing 100% pure hcp titanium. The strain originating from the deposition process is manifested by slightly broader peaks toward the high detection angles.....	33

## 7 References

- [1] KETOLA, Jonne Jalmari. *Cold sprayed coatings in biomedicine*. 2014. Master's Thesis.
- [2] WANG, Q.; ZHANG, M. Cold-spray coatings on magnesium and its alloys. In: *Surface Modification of Magnesium and its Alloys for Biomedical Applications*. Woodhead Publishing, 2015. p. 379-405.
- [3] XIE, Yingchun, et al. Formation mechanism and microstructure characterization of nickel-aluminum intertwining interface in cold spray. *Surface and Coatings Technology*, 2018, 337: 447-452.
- [4] HUSSAIN, T. Cold spraying of titanium: a review of bonding mechanisms, microstructure and properties. In: *Key engineering materials*. Trans Tech Publications Ltd, 2013. p. 53-90.
- [5] YIN, Shuo, et al. Formation conditions of vortex-like intermixing interfaces in cold spray. *Materials & Design*, 2021, 200: 109444.
- [6] HEIMANN, Robert B.; LEHMANN, Hans D. *Bioceramic coatings for medical implants: trends and techniques*. John Wiley & Sons, 2015.
- [7] NOORAKMA, Abdullah CW, et al. Hydroxyapatite-coated magnesium-based biodegradable alloy: cold spray deposition and simulated body fluid studies. *Journal of materials engineering and performance*, 2013, 22.10: 2997-3004.
- [8] SCHMIDT, Tobias, et al. From particle acceleration to impact and bonding in cold spraying. *Journal of thermal spray technology*, 2009, 18.5: 794-808.
- [9] PAPYRIN, Anatolii, et al. *Cold spray technology*. Elsevier, 2006.
- [10] BANDAR, AL-Mangour, et al. Improving the strength and corrosion resistance of 316L stainless steel for biomedical applications using cold spray. *Surface and Coatings Technology*, 2013, 216: 297-307.
- [11] HENCH, Larry L. Biomaterials: a forecast for the future. *Biomaterials*, 1998, 19.16: 1419-1423.
- [12] WU, Guosong; IBRAHIM, Jamesh Mohammed; CHU, Paul K. Surface design of biodegradable magnesium alloys—a review. *Surface and Coatings Technology*, 2013, 233: 2-12.
- [13] MONSALVE, M., et al. Bioactivity and mechanical properties of plasma-sprayed coatings of bioglass powders. *Surface and Coatings Technology*, 2013, 220: 60-66.
- [14] SINGH, R. P. Numerical evaluation, optimization and mathematical validation of cold spraying of hydroxyapatite using taguchi approach. *Inter J Eng Sci Technol*, 2011, 3: 7006-7015.
- [15] KHODABAKHSHI, Farzad, et al. Interfacial bonding mechanisms between aluminum and titanium during cold gas spraying followed by friction-stir modification. *Applied Surface Science*, 2018, 462: 739-752.
- [16] GRUJICIC, Mica, et al. Analysis of the impact velocity of powder particles in the cold-gas dynamic-spray process. *Materials Science and Engineering: A*, 2004, 368.1-2: 222-230.
- [17] CHEN, Chaoyue, et al. Metallization of polyether ether ketone (PEEK) by copper coating via cold spray. *Surface and Coatings Technology*, 2018, 342: 209-219.